KSME

Springer

Journal of Mechanical Science and Technology 37 (12) 2023

Original Article
DOI 10.1007/s12206-023-1138-6

Keywords:
· Parallel mechanism
· Type synthesis
· Actuation wrench screw theory
· Fully-decoupled
· Mobility

Correspondence to:
Yanbin Zhang
yanbin_zh@haust.edu.cn

Citation:
Zhang, Y., Wei, X., Zhang, S., Chang, Z., Li, Y. (2023). Type synthesis of the fully-decoupled two-rotational and one-translational parallel mechanism. Journal of Mechanical Science and Technology 37 (12) (2023) 6669~6678.
http://doi.org/10.1007/s12206-023-1138-6

Received December 20th, 2022
Revised May 16th, 2023
Accepted September 8th, 2023

† Recommended by Editor Ja Choon Koo

Type synthesis of the fully-decoupled two-rotational and one-translational parallel mechanism

Yanbin Zhang[1,2], Xuemin Wei[1], Shuang Zhang[1,2], Zhenzhen Chang[1] and Yaoguang Li[1]

[1]School of Mechatronics Engineering, Henan University of Science and Technology, Luoyang 471003, China, [2]Center of Machinery Equipment Advanced Manufacturing of Henan Province, Luoyang 471003, China

Abstract Type synthesis of parallel mechanism is regarded as the theoretical basis and source for the original innovation design of mechanical devices and robots. A new method for type synthesis of the fully-decoupled two-rotational and one-translational (2R1T) parallel mechanisms with three degrees of freedom is proposed in this paper. Based on the actuation wrench screw theory, the mathematical model mapping the input and output velocity vector space of the fully-decoupled 2R1T parallel mechanism is established. The actuation wrench screws and the actuated twist screws of the corresponding branches are derived according to the mathematic model. The forms of the unactuated screws are determined in terms of the reciprocal product theory. Structural synthesis of the branch chains is realized. Then type synthesis of parallel mechanisms is completed as well and lots of novel mechanisms are obtained. Finally, a 2RUPU-PU parallel mechanism synthesized is taken as an example to analyze its mobility and kinematics. Results show that the mechanism has two-rotational and one-translational degrees of freedom and its Jacobian matrix is a diagonal matrix, i.e., it has the fully-decoupled kinematic characteristics. Therefore, the method proposed is correct and effective to synthesize the fully-decoupled 2R1T parallel mechanisms.

1. Introduction

Parallel robotic mechanism is composed of multiple closed-loop structures, and at least two branch kinematic chains are required to connect the moving platform to the basic platform. It has the advantages of compact structure, high stiffness, small motion inertia, and fast response speed. Recently, parallel mechanism has been widely used in multiple fields, such as parallel machine tools, industrial robots, medical robots, force sensors, and so on.

Theoretical base and source for unique innovation design of mechanical devices and robotics is considered to be type synthesis of parallel mechanism (PM). It is a challenging problem in the fields of mechanism and robotics. At the early stage, to synthesize PMs, the enumeration approach based on the degree of freedom formula was applied [1, 2]. Although this method is intuitive and simple, there are many problems in the design of over constrained PMs. Recently, some new mathematical theories were introduced into type synthesis of PMs, and a few of approaches have been presented, such as the displacement subgroup theory based method [3-5], the constraint screw theory based method [6, 7], the linear transformation theory based method [8-10], the position orientation characteristic (POC) set based method [11, 12] and the GF set based method [13-15]. Each method has its own properties and model for constructing the novel PMs with differently structural and kinematical characteristics.

Lower-mobility PMs have become research and application hotspots due to their simple structure, convenient manufacture, ease to control and low maintenance costs. Parallel mechanisms with 3-DOF have been payed the most attention by the global scholars during the past two decades [16-18]. There are four types of 3-DOF PMs, i.e., three-translational (3T), three-rotational (3R), two-rotational and one-translational (2R1T), and two-translational and one-rotational (2T1R). Among them, 2R1T parallel mechanism with the mixed rotational and translational motion can be used in radar antennas, rehabilitation robots and parallel machine tools, etc. 3RPS parallel mechanism is the most typical one [19]. In addition, Choi [20] presented a (2-RRU)-URR over constrained 2R1T PMs, which can be applied to the human thumb rehabilitation device. Herrero [21] proposed a 2PRU-1PRS 2R1T multi-axis vibration table, which can be applied to the inspection of auto parts. Sun [22] performed type synthesis of 2R1T PM with parasitic motion based on the finite motion screw method. Xu [23] synthesized a family of 2R1T PMs based on the ultimate constraint wrenches. Qin [24] designed a kind of 2R1T PMs without parasitic motion. Wu [25] proposed a 2R1T redundant parallel mechanism with a larger workspace and higher motion/force transfer performance based on Lie group method.

To do so reduce the high motion coupling and increase the workspace, decupled or isotropic PMs have been created. For these mechanisms, their velocity Jacobian matrix may be a triangular, or a diagonal, even an identity matrix. As a result, the mapping relationship between the moving platform's output velocity space and the input velocity space of the actuated joints is fairly straightforward. Finding their kinematics analytical solution is quite simple. Gogu [26, 27] discussed type composition of the fully-isotropic PMs using the linear transformation theory. Carricato [28] presented synthesis of fully-isotropic 3T1R-type PMs. Kuo and Dai [29] performed structure synthesis of PMs with fully decupled projective motion, a class of decoupled PMs with 2-, 3-, 4-, 5-, and 6-DOF were achieved. Zhang [30, 31] completed type synthesis of the uncoupled spatial translational and two-DOF rotational PM per the theory of the actuation wrench screw. In addition, a lot of novel decoupled parallel mechanisms were designed [32-34], which could be applied in industrial equipment and robots due to their well motion/force transmission performances.

This work put forward a systematic method with regard to determine the kind of a class of fully-decoupled 2R1T PMs, which is per the branch actuation wrench screw theory. Firstly, motion mathematic model of the fully-decoupled 2R1T PM is set up in Sec. 2. Determination of the branch actuation wrench screws, the actuated screws and the unactuated screws, and structural synthesis of the branch chains are all performed in next two sections, type synthesis of the completely decoupling 2R1T PM is conducted, and a lot of novel mechanisms are obtained as well. Then, mobility and kinematics analysis of a 2RUPU-PU mechanism synthesized are discussed in Sec. 5, which demonstrates the fully-decoupled feature of the PM and verifies the validity of the approach presented here. Finally, some conclusions are given in Sec. 6.

2. Mathematic motion model of the fully-decoupled 2R1T PM

For the n-DOF PMs, the moving platform's velocity equation may be stated as

$$\mathbf{T}=\sum_{j=1}^{F_i}\dot{q}_{ji}\$_{ji}\left(i=1,2,...,n\right) \tag{1}$$

where, $\mathbf{T}$ is the instantaneous output velocity vector of the moving platform, $\dot{q}_{ji}$ and $\$_{ji}$ denote the instantaneous velocity the corresponding motion screw of the *j*-th joint in the *i*-th branch, respectively, F_i represents the connectivity of the *i*-th branch, n denotes the sum of branches.

Using both sides of Eq. (1) to produce the reciprocal product, utilizing the actuation wrench screw of the i-th branch, we get

$$\$_{ai}\circ\mathbf{T}=\dot{q}_{1i}\$_{ai}\circ\$_{1i}\left(i=1,2,...,n\right) \tag{2}$$

where, $\$_{ai}=[L_{ai}\quad M_{ai}\quad N_{ai};P_{ai}\quad Q_{ai}\quad R_{ai}]^{\mathrm{T}}$, is the actuation wrench screw of the *i*-th branch, $\$_{1i}$ represents the twist screw of the actuated joint, $\dot{q}_{1i}$ is the instantaneous velocity corresponding to the screw $\$_{1i}$.

Rewriting Eq. (2) into the matrix form, have

$$\mathbf{J}_{dir}V=\mathbf{J}_{inv}\dot{\mathbf{q}} \tag{3}$$

where, $V=[\boldsymbol{\omega};\mathbf{v}]^{\mathrm{T}}=[\omega_x\quad\omega_y\quad\omega_z;\ v_x\quad v_y\quad v_z]^{\mathrm{T}}$, is the velocity vector of the moving platform, $\boldsymbol{\omega}$ and $\mathbf{v}$ are the output angular velocity vector and linear velocity vector, respectively, $\dot{\mathbf{q}}=[\dot{q}_{11}\quad\dot{q}_{12}\cdots\cdots\dot{q}_{1n}]^{\mathrm{T}}$ the vector of input velocity of the $\$_{1i}$, $\mathbf{J}_{dir}$ the direct Jacobian matrix, which is composed of the branch actuation wrench screws of all branches, $\mathbf{J}_{inv}$ the inverse Jacobian matrix, which is a diagonal matrix. The non-zero diagonal components are the reciprocal product of the $\$_{ai}$ and $\$_{1i}$, and have

$$\mathbf{J}_{dir}=\begin{bmatrix}\$_{a1}^{\mathrm{T}}\\\$_{a2}^{\mathrm{T}}\\\vdots\\\$_{an}^{\mathrm{T}}\end{bmatrix}=\begin{bmatrix}L_{a1}&M_{a1}&N_{a1}&P_{a1}&Q_{a1}&R_{a1}\\L_{a2}&M_{a2}&N_{a2}&P_{a2}&Q_{a2}&R_{a2}\\\vdots&\vdots&\vdots&\vdots&\vdots&\vdots\\L_{an}&M_{an}&N_{an}&P_{an}&Q_{an}&R_{an}\end{bmatrix}_{n\times6} \tag{4}$$

$$\mathbf{J}_{inv}=\begin{bmatrix}\$_{a1}\circ\$_{11}&0&\cdots&0\\0&\$_{a2}\circ\$_{12}&\cdots&0\\\vdots&\vdots&\ddots&\vdots\\0&0&\cdots&\$_{an}\circ\$_{1n}\end{bmatrix}_{n\times n} \tag{5}$$

Since $\mathbf{J}_{inv}$ is a diagonal matrix, if a mechanism possesses the fully-decoupled feature, $\mathbf{J}_{dir}$ must be also a diagonal matrix. Therefore, the key step to establish type synthesis method of the fully-decoupled 2R1T PMs built on Eq. (3) lies in how to determine the forms of all branch actuation wrench screws $\$_{ai}$.

Assuming PMs proposed in this paper only have two rotational DOFs around the *z*-and *x*-axis direction, respectively, and one translational DOF along the y-axis direction, so we have v_x = 0, v_z = 0 and ω_y = 0. Ref. [30] pointed out that the actuation wrench screws of the fully-decoupled PM with two rotational DOFs, which independently control the rotational motion of the moving platform, one is a zero-pitch wrench screw (i.e., linear force vector), another is an infinite-pitch wrench screw (i.e., pure couple vector). Without loss generality, it is assumed that the actuation wrench screws are a linear force vector and a couple vector, respectively, the moving platform is independently controlled to rotate around the *x*- and *z*-axis. However, the actuation wrench screw that independently drives the platform to move along the y-axis direction, must be a zero-pitch screw [31]. Thus, referring Eq. (4), the direct Jacobian matrix of the 2R1T PM can be derived as follows

$$\mathbf{J}_{dir}=\begin{bmatrix} L_{a1} & M_{a1} & N_{a1}; & P_{a1} & Q_{a1} & R_{a1} \\ 0 & 0 & 0; & L_{a2} & M_{a2} & N_{a2} \\ L_{a3} & M_{a3} & N_{a3}; & P_{a3} & Q_{a3} & R_{a3} \end{bmatrix} \tag{6}$$

If removing the zero elements in vector $\mathbf{V}$ in Eq. (3) and the corresponding column in $\mathbf{J}_{dir}$ in Eq. (6), the velocity equation of 2R1T PM can be obtained as

$$\begin{bmatrix} P_{a1} & R_{a1} & M_{a1} \\ L_{a2} & N_{a2} & 0 \\ P_{a3} & R_{a3} & M_{a3} \end{bmatrix}\begin{bmatrix} \omega_x \\ \omega_z \\ v_y \end{bmatrix}=\begin{bmatrix} \varsigma_1 & 0 & 0 \\ 0 & \varsigma_2 & 0 \\ 0 & 0 & \varsigma_3 \end{bmatrix}\begin{bmatrix} \dot{q}_{11} \\ \dot{q}_{12} \\ \dot{q}_{13} \end{bmatrix} \tag{7}$$

where, $\varsigma_i = \$_{ai} \circ \$_{1i}\ (i = 1, 2, 3)$.

For a fully-decoupled PM, the corresponding relationship between the output speed and the input speed corresponds to each other. So the mathematic motion model of the fully-decoupled 2R1T PM will be achieved, and

$$\begin{bmatrix} P_{a1} & 0 & 0 \\ 0 & N_{a2} & 0 \\ 0 & 0 & M_{a3} \end{bmatrix}\begin{bmatrix} \omega_x \\ \omega_z \\ v_y \end{bmatrix}=\begin{bmatrix} \varsigma_1 & 0 & 0 \\ 0 & \varsigma_2 & 0 \\ 0 & 0 & \varsigma_3 \end{bmatrix}\begin{bmatrix} \dot{q}_{11} \\ \dot{q}_{12} \\ \dot{q}_{13} \end{bmatrix}. \tag{8}$$

If the direct Jacobian matrix in Eq. (8) is full rank, Jacobian matrix of mechanism is

$$\boldsymbol{J}=\boldsymbol{J}_{dir}^{-1}\boldsymbol{J}_{inv}=\begin{bmatrix} \varsigma_1/P_{a1} & 0 & 0 \\ 0 & \varsigma_2/N_{a2} & 0 \\ 0 & 0 & \varsigma_3/M_{a3} \end{bmatrix} \tag{9}$$

and

$$\boldsymbol{J}_{dir}=\begin{bmatrix} P_{a1} & 0 & 0 \\ 0 & N_{a2} & 0 \\ 0 & 0 & M_{a3} \end{bmatrix} \tag{10}$$

$$\boldsymbol{J}_{inv}=\begin{bmatrix} \varsigma_1 & 0 & 0 \\ 0 & \varsigma_2 & 0 \\ 0 & 0 & \varsigma_3 \end{bmatrix}. \tag{11}$$

3. Structural synthesis of branches for the fully-decoupled 2R1T parallel mechanism

Key work for the structural synthesis of branches is to define the quantity and the type of the possible joints, and their assembly order in the branches.

Establish a static coordinate system o-xyz, with its coordinate origin o located on the basic platform; In the moving coordinate system O-XYZ, the origin O is fixedly connected to the moving platform, and the three coordinate axes of the two coordinate systems correspond to parallel at the initial position, as shown in Fig. 1.

3.1 The first branch chain

3.1.1 Determination of the actuation wrench screw

Assuming the first branch chain independently controls the platform to rotate around *x*-axis. Referring to Eqs. (6)-(8), it can be known that the $\$_{a1}$ of the first branch should be a zero-pitch screw perpendicular to *y*-axis. Therefore, branch actuation wrench screw $\$_{a1}$ can be written as

$$\$_{a1}=[L_{a1}\quad 0\quad N_{a1};\quad P_{a1}\quad Q_{a1}\quad 0]^{\mathrm{T}}. \tag{12}$$

In Eq. (12), the component P_{a1} is non-zero, then the component L_{a1} of $\$_{a1}$ on *x*-axis can be determined. So the form of $\$_{a1}$ is derived as

$$\$_{a1}=[0\quad 0\quad 1;\quad P_{a1}\quad Q_{a1}\quad 0]^{\mathrm{T}}. \tag{13}$$

Eq. (13) shows that $\$_{a1}$ is a zero-pitch wrench screw, and its direction is parallel to *z*-axis, as show in Fig. 1.

3.1.2 Determination of the actuated twist screw

In terms of the first element on the diagonal of the $\mathbf{J}_{inv}$ in Eq. (11) must be non-zero, we get

$$\varsigma_1 = \$_{a1} \circ \$_{11} \neq 0 \tag{14}$$

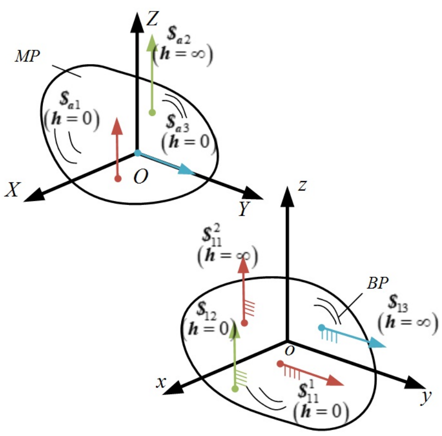

Fig. 1. Actuation wrench screws and actuation twist screws of mechanism branches.

where $\mathbf{\$}_{11}$ is the actuated twist screw of the first branch, which has two forms.

Case I, when $\mathbf{\$}_{11}$ is a zero-pitch twist screw.

The form of $\mathbf{\$}_{11}^{1}$ can be written as

$$\mathbf{\$}_{11}^{1} = [L_{11} \quad M_{11} \quad N_{11}; \quad P_{11} \quad Q_{11} \quad R_{11}]^{\mathrm{T}} . \tag{15}$$

Simultaneous Eqs. (13)-(15), we obtain

$$\varsigma_1 = R_{11} + P_{a1}L_{11} + Q_{a1}M_{11} . \tag{16}$$

From Eq. (16), it can be seen that the value of ς_1 is only related to the components L_{11}, M_{11} and R_{11}, so we have $N_{11} = P_{11} = Q_{11}$ = 0. Simultaneously, in order to ensure that the condition ς_1 = 0 is always satisfied, at least one of the components L_{11} and M_{11} of $\mathbf{\$}_{11}$ on the *x*-axis and *y*-axis directions should be non-zero. No loss generality, we take L_{11} = 0 and M_{11} = 1. Then, the form of the $\mathbf{\$}_{11}^{1}$ is

$$\mathbf{\$}_{11}^{1} = [0 \quad 1 \quad 0; \quad 0 \quad 0 \quad R_{11}]^{\mathrm{T}} . \tag{17}$$

The first branch's $\mathbf{\$}_{11}^{1}$ is obviously screw with zero-pitch parallel to the y-axis, as show in Fig. 1. Therefore, the actuated joint of the first branch can be a rotational joint, and its installation direction on the base is parallel to y-axis.

Case II, when $\mathbf{\$}_{11}$ is an infinite-pitch screw.

In this condition, the form of $\mathbf{\$}_{11}^{2}$ is

$$\mathbf{\$}_{11}^{2} = [0 \quad 0 \quad 0; \quad L_{11} \quad M_{11} \quad N_{11}]^{\mathrm{T}} . \tag{18}$$

Similarly

$$\varsigma_1 = N_{11} . \tag{19}$$

Eq. (19) shows that ς_1 is only related to the component of the actuated twist screw $\mathbf{\$}_{11}$ on the *z*-axis, and has nothing to do with other components (L_{11} and M_{11}). So the form of $\mathbf{\$}_{11}^{2}$ can be taken as

$$\mathbf{\$}_{11}^{2} = [0 \quad 0 \quad 0; \quad 0 \quad 0 \quad 1]^{\mathrm{T}} . \tag{20}$$

As a result, the first branch's actuated twist screw can likewise be an infinite-pitch screw with an axis parallel to the z-axis, as show in Fig. 1. Thus, the prismatic joint can be chosen as the actuated joint of the first branch, which is installed on the fixed and has a direction parallel to the z-axis.

3.1.3 Determination of the unactuated screws

Class I, when $\mathbf{\$}_{11}$ is a zero-pitch screw.

According to the condition that the reciprocal product of the actuation wrench screw and all other twist screws except for the actuated screw in the same branch is always equal to zero, the following is how the shapes of all unactuated screws can be determined:

I-1, zero-pitch screw parallel to *y*-axis. The number is one and only one. It indicates that the rotational joint parallel to *y*-axis can be selected as the non-actuated joint of the first branch. In addition, this joint must be directly connected with the actuated joint.

I-2, screw whose axis is parallel to the z-axis and whose pitch is zero. Its number is at least one and at most three. In other words, the rotational joints parallel to *z*-axis can be chosen as the non-actuated joint.

I-3, infinite-pitch screw whose axis is normal to *z*-axis. Its number is at most 2 and the screws are not parallel to each other. So the prismatic pair perpendicular to *z*-axis can be taken as the active joints.

I-4, zero-pitch screw parallel to the *x*-axis. its number is one and only one. It is only fixed to the moving platform.

Class II, when $\mathbf{\$}_{11}$ is an infinite-pitch screw.

Similarly, based on the reciprocal product principle, the feasible unactuated screws will be also determined as follows.

II-1, the screw parallel to *z*-axis and pitch is zero. There is at least one and not more than three zero-pitch screws in the branch.

II-2, zero-pitch screw parallel to the *x*-axis. It intersects the axis of the $\mathbf{\$}_{a1}$ and its number is one and only one. Moreover, it is only located at the end of the branch and directly assembled on the moving platform.

II-3, infinite-pitch screw normal to *z*-axis. It is no more than two and their axes are perpendicular to the *z*-axis.

II-4, zero-pitch screw parallel to *y*-axis. The number is not more than one. It is worth noting that it is an idle screw, and its position unable to intersect two parallel zero-pitch screws.

3.1.4 Structural synthesis of the first branch

After determining the kinds of the actuated twist screws and all unactuated screws, the type and the assembling orientation of the actuated joint and the possible unactuated joints for the branches will be determined. Then, based on the different connectivity (C_n), all feasible branch structure can be listed, as shown in Tables 1 and 2. Table 1 exhibits when the actuated twist screw is zero-pitch, the branch connectivity can only be 6. The branch chain has three basic types, 4R2P-, 5R1P- and 6R-type. If the actuated screw is infinite-pitch, the branch connectivity will be 5 and 6. There are 6 basic branch types, such as 2R3P, 3R2P, 4R1P, 3R3P, 4R2P and 5R1P, shown in Table 2.

In Tables 1 and 2, the subscript letters x, y, z express the corresponding joint's axis direction at the initial position. If two or more joints have the same right subscript letter, which indicates that the relative joints are parallel to one another. Otherwise, they are perpendicular. The axis direction of the prismatic pair with subscript *m* is perpendicular to the axes of the adjacent rotational joints. If the first joint in the branch is a cylindrical joint (C joint), the superscript letter *r* or *t* is used to present its angular displacement or linear displacement selected as the actuated input. The letter X shows that the corresponding joint

Table 1. Structural forms of the first branch when the actuated screw is zero-pitch.

C_n	Type	The basic branch forms	Branches with multi-DOF joints
6	4R2P	$R_yR_yP_xP_yR_zR_x$	$R_yR_yP_xP_yU_{xz}$
		$R_yR_yR_zP_xP_yR_x$	$R_yU_{yz}P_xP_yR_x$
		$R_yR_yP_xR_zP_yR_x$	$R_yC_yP_xU_{xz}$
		$R_yP_yR_yP_xR_zR_x$	$R_yC_yR_zP_xR_x$
		$R_yP_yR_yR_zP_xR_x$	
	5R1P	$R_yR_yP_xR_zR_zR_x$	$R_yR_yP_xR_zU_{xz}$
		$R_yR_yR_zP_xR_zR_x$	$R_yU_{yz}P_mU_{zx}$
		$R_yR_yR_zR_zP_xR_x$	$R_yR_yR_zR_zC_x$
		$R_yR_yR_zR_zR_xP_x$	$R_yU_{yz}R_zC_x$
	6R	$R_yR_yR_zR_zR_zR_x$	$R_yU_{yz}R_zU_{zx}$

Table 2. Structural forms of the first branch when the actuated screw is infinite pitch.

C_n	Type	The basic branch forms	Branches with multi-DOF joints
5	2R3P	$P_zR_zP_xP_yR_x$	$C_z^tP_xP_yR_x$
		$P_zP_xR_zP_yR_x$	
		$P_zP_xP_yR_zR_x$	$P_zP_xP_yU_{xz}$
	3R2P	$P_zP_mR_zR_zR_x$	$P_zP_mR_zU_{xz}$
		$P_zR_zP_mR_zR_x$	Ct zP_mU_{zx};$C_zP_mU_{xz}$
		$P_zR_{zRz}P_mR_x$	Ct $zR_zP_mR_x$
	4R1P	$P_zR_zR_zR_zR_x$	$C_z^tR_zR_zR_x$;$C_zR_zU_{xz}$
6	3R3P	$P_zP_xP_yR_yR_zR_x$	$P_zP_xP_yS$;$P_zP_xC_yU_{xz}$
		$P_zP_xR_yR_zP_yR_x$	$P_zP_xU_{yz}P_yR_x$
		$P_zR_yR_zP_xP_yR_x$	$P_zU_{yzPx}P_yR_x$
	4R2P	$P_zP_xR_zR_zR_yR_x$	$P_zP_xR_zR_zU_{yz}$
		$P_zR_zP_mR_zR_yR_x$	$C_z^tP_mR_zU_{xy}$;C_zP_mS
		$P_zR_zR_zP_mR_yR_x$	$C_z^tR_zP_mU_{xy}$
		$P_zR_yP_mR_zR_zR_x$	$P_zR_yP_mR_zU_{xz}$
		$P_zR_yR_zP_mR_zR_x$	$P_zU_{yz}P_mU_{xz}$
		$P_zR_yR_zR_zP_mR_x$	$P_zU_{yz}R_zP_mR_x$
	5R1P	$P_zR_zR_zR_zR_yR_x$	$C_z^tR_zR_zU_{xy}$
		$P_zR_yR_zR_zR_zR_x$	$P_zR_yR_zR_zU_{xz}$

is an idle one.

3.2 The second branch chain

3.2.1 Determination of the actuation wrench screw

The platform's rotation around the z-axis can be independently controlled by the second branch chain, what's more, the main thrust applied to the base by the branch-actuated joint is a couple vector, i.e., an infinite-pitch screw, $\$_{a2}$. Therefore, we have

$$\$_{a2}=[0 \quad 0 \quad 0;\quad L_{a2} \quad M_{a2} \quad N_{a2}]^{\mathrm{T}} . \tag{21}$$

According to Eqs. (7) and (10), the direct Jacobian $\boldsymbol{J}_{dir}$ is diagonal matrix, all components in the second row are equal to zero except for N_{a2}, so the form of $\$_{a2}$ is

$$\$_{a2}=[0 \quad 0 \quad 0;\quad 0 \quad 0 \quad 1]^{\mathrm{T}} . \tag{22}$$

It can be known from Eq. (22) that the $\$_{a2}$ of the second branch is an infinite-pitch screw whose direction is in the same direction as the z-axis, as show in Fig. 1.

3.2.2 Determination of the actuated twist screw

By means of the condition that the second component in Jacobian $\mathbf{J}_{inv}$ is non-zero, yields

$$\varsigma_2 = \$_{a2} \circ \$_{12} \neq 0 . \tag{23}$$

Since the reciprocal product of any two infinite-pitch screws is always equal to zero, then the second branch actuated twist screw can only be a zero-pitch screw, and let

$$\$_{12} = [L_{12} \quad M_{12} \quad N_{12};\quad P_{12} \quad Q_{12} \quad R_{12}]^{\mathrm{T}} . \tag{24}$$

Substituting Eqs. (22) and (24) into Eq. (23), we have

$$\varsigma_2 = N_{12} . \tag{25}$$

Eq. (25) demonstrates that, the ς_2 is only related to the component N_{12} of the z-axis direction vector of the actuated twist screw $\$_{12}$, but independent of its components L_{12} and M_{12}, so we have $L_{12} = M_{12} = 0$, $N_{12} = 1$. Then, the form of $\$_{12}$ is

$$\$_{12}=[0 \quad 0 \quad 1;\quad 0 \quad 0 \quad 0]^{\mathrm{T}} . \tag{26}$$

It is obvious that the actuated joint of the second branch is a rotational joint, and its installation orientation on the fixed base is parallel to *z*-axis, as show in Fig. 1.

3.2.3 Determination of the unactuated screws

Similarly, the possible unactuated screws can be ascertained as follows.

1) Zero-pitch screw in the same direction as the *x*-axis. Its number is not more than three.

2) Zero-pitch screw in the same direction as the *y*-axis. The number is also not more than three.

3) Infinite-pitch screw. The number is at most two along any direction.

3.2.4 Structural synthesis of the second branch

In accordance with difference in connectivity, the feasible structural forms of the second branch can be listed, as shown in Table 3. There are five basic types, 3R2P, 4R1P, 4R2P, 5R1P and 6R.

Table 3. Structural forms of the second branch.

C_n	Type	The basic branch forms	Branches with multi-DOF joints
5	3R2P	$R_zP_xR_xP_mR_x$	$R_zC_xP_mR_x$
		$R_zR_xP_mR_xP_x$	$R_zR_xP_mC_x$
		$R_zP_zR_xR_xP_x$	$C_z^rR_xR_xP_x;C_zR_xC_x$
		$R_zR_xR_xP_zP_x$	$U_{zx}zR_xP_zP_x$
		$R_zP_xR_xR_xP_z$	$R_zC_xR_xP_z$
		$R_zP_xP_zR_xR_x$	
	4R1P	$R_zP_mR_xR_xR_x$	$R_zC_xR_xR_x$
		$R_zR_xR_xR_xP_x$	$R_zR_xR_xC_x;U_{zx}R_xC_x$
6	4R2P	$R_zR_yP_xR_xP_zR_x$ $R_zP_xR_yR_xP_zR_x$	$R_zR_yC_xP_zR_x$
			$R_zP_xU_{xy}P_zR_x$
		$R_zP_xR_xP_zR_xR_y$	$R_zC_xP_zU_{xy}$
		$R_zR_xP_zR_xP_xR_y$	$U_{zx}P_zC_xR_y$
		$R_zR_yR_xP_zR_xP_x$	$R_zU_{xy}P_zC_x$
		$R_zR_xP_zR_xR_yP_x$	$R_zR_xP_zU_{xy}P_x$
		$R_zP_zR_xR_xR_yP_x$	$C_z^rR_xU_{xy}P_x$
		$R_zR_yP_zR_xR_xP_x$	$R_zR_yP_zR_xC_x$
		$R_zP_zR_xR_xP_xR_y$	$C_z^rR_xC_xR_y$
		$R_zR_xR_xP_zR_yP_x$	$U_{zx}R_xP_zR_yP_x$
		$R_zR_xR_xP_zP_xR_y$	$U_{zx}R_xP_zP_xR_y$
		$R_zR_yR_xR_xP_zP_x$	$R_zU_{xy}R_xP_zP_x$
		$R_zR_yP_xR_xR_xP_z$	$R_zR_yC_xR_xP_z$
		$R_zP_xR_yR_xR_xP_z$	$R_zP_xU_{xy}R_xP_z$
		$R_zP_xR_xR_xP_zR_y$	$R_zC_xR_xP_zR_y$
		$R_zR_yP_xP_zR_xR_x$	$U_{zy}P_xP_zR_xR_x$
		$R_zP_xP_zR_xR_xRy$	$R_zP_xP_zR_xU_{xy}$
		$R_zP_xR_yP_zR_xR_x$	
	5R1P	$R_zR_yP_xR_xR_xR_x$	$U_{zy}C_xR_xR_x$
		$R_zP_mR_yR_xR_xR_x$	$R_zP_mU_{xy}R_xR_x$
		$R_zP_mR_xR_xR_xR_y$	$R_zC_xR_xU_{xy}$
		$R_zR_yR_xR_xR_xP_x$	$R_zU_{xy}R_xC_x$
		$R_zR_xR_xR_xR_yP_x$	$R_zR_xR_xU_{xy}P_x$
		$R_zR_xR_xR_xP_xR_y$	$R_zR_xR_xC_xR_y$
		$R_zR_xR_yP_mR_yR_x$	$R_zU_{xy}P_mU_{yx}$
		$R_zP_mR_yR_yR_yR_x$	$R_zC_yR_yU_{yx}$
		$R_zR_yP_mR_yR_yR_x$	$R_zR_yC_yU_{yx}$
		$R_zR_yR_yP_mR_yR_x$	$R_zR_yR_yC_yR_x$
		$RzR_yR_yR_yP_mR_x$	$R_zR_yR_yC_yR_x$
	6R	$R_zR_xR_xR_xR_yR_y$	$U_{zx}R_xU_{xy}R_y$
		$R_zR_xR_xR_yR_yR_x$	$R_zR_xU_{xy}R_yR_x$
		$R_zR_xR_yR_yR_xR_x$	$R_zU_{xy}R_yR_xR_x$
		$R_zR_yR_yR_xR_xR_x$	$R_zR_yU_{yx}R_xR_x$
		$R_zR_yR_yR_yR_xR_x$	$R_zR_yR_yU_{yx}R_x$
		$R_zR_yR_yR_xR_xR_y$	$R_zR_yR_yR_xU_{xy}$
		$R_zR_yR_xR_xR_yR_y$	$R_zR_yR_xU_{xy}R_y$
		$R_zR_yR_yR_xR_yR_x$	$R_zR_yR_yU_{xy}R_x$
		$R_zR_xR_yR_yR_yR_x$	$R_zU_{xy}R_yU_{yx}$

3.3 The third branch chain

3.3.1 Determination of the actuation wrench screw

Provided that the third branch controls independently the platform to translate along *y*-axis. Based on the analysis mentioned above, the actuation wrench screw of the third branch must be a linear force vector.

Referring to Eqs. (7) and (10), if direct Jacobian matrix $\boldsymbol{J}_{dir}$ is full rank, only component M_{a3} is non-zero in the third row. Therefore, the form of the $\$_{a3}$ is obtained as follows

$$\$_{a3}=[0 \quad 1 \quad 0; \quad 0 \quad 0 \quad 0]^{\mathrm{T}} . \tag{27}$$

Eq. (27) shows that $\$_{a3}$ is parallel to the *y*-axis, as show in Fig. 1.

3.3.2 Determination of the actuated twist screw $\$_{13}$

Case 1, when $\$_{13}$ is an infinite-pitch screw.

The form of the $\$_{13}$ is

$$\$_{13}=[0 \quad 0 \quad 0; \quad L_{13} \quad M_{13} \quad N_{13}]^{\mathrm{T}} . \tag{28}$$

Since the component ς_3 in Eq. (10) should be non-zero, then

$$\varsigma_3=\$_{a3} \circ \$_{13} \neq 0 . \tag{29}$$

Substituting Eqs. (27) and (28) into Eq. (29), can get

$$\varsigma_3=M_{13} . \tag{30}$$

Apparently, the value of ς_3 is only related to the component M_{13} of direction vector of the actuated twist screw on the *y*-axis, and has nothing to do with the components on other axes. So we can take $L_{13}=N_{13}$ = 0, M_{13} = 1. Then, have

$$\$_{13}=[0 \quad 0 \quad 0; \quad 0 \quad 1 \quad 0]^{\mathrm{T}} . \tag{31}$$

Eq. (27) shows that $\$_{13}$ is an infinite-pitch screw in the same direction as *y*-axis, as show in Fig. 1. Additionally, it is determined that the y-axis-installed actuated joint of the third branch is a prismatic pair.

Case 2, when the $\$_{13}$ is a zero-pitch screw.

In this case, the form of $\$_{13}$ can be written as

$$\$_{13}=[L_{13} \quad M_{13} \quad N_{13}; \quad P_{13} \quad Q_{13} \quad R_{13}]^{\mathrm{T}} . \tag{32}$$

Substitute Eqs. (22) and (32) into Eq. (29), yields

$$\varsigma_3=Q_{13} . \tag{33}$$

Due to the value of ς_3 is exclusively linked to the screw component Q_{13}, other components can be taken as $L_{13}=M_{13}=N_{13}$ = 0 and $P_{13}=R_{13}$ = 0. This is contrary to the assump-

Table 4. Structural forms of the third branch.

C_n	Type	The basic branch forms	Branches with multi-DOF joints
3	2R1P	$P_yR_zR_x$	P_yU_{zx}
4	3R1P	$P_yR_yR_zR_x$	$C_y^tR_zR_x$;$P_yR_yU_{zx}$
		$P_yR_zR_yR_x$	$P_yU_{zy}R_x$
		$P_yR_zR_xR_y$	$P_yR_zU_{xy}$;P_yS

tion that $\$_{13}$ is a zero-pitch screw. Therefore, $\$_{13}$ only is an infinite-pitch screw.

3.3.3 Determination of the unactuated screws

Similarly, the forms of all unactuated screws will be obtained as follows.

1) Zero-pitch screw that is parallel to *x*-axis. There is one and only one, and at the end of the branch chain.

2) Zero-pitch screw parallel to *z*-axis. The number is also only one.

3) Zero-pitch screw whose axis is parallel to *y*-axis. There is not more than one and it is an idle screw.

4) Infinite-pitch screw parallel to *x*-axis. Its number is not more than one as well.

3.3.4 Structural synthesis of the branch

On the basis of the forms of actuated twist screws and the unactuated screws obtained, all feasible structures for the third branch be synthesized, as shown in Table 4. There are only two basic types, i.e., 2R1P and 3R1P.

4. The fully-uncoupled 2R1T parallel mechanism

After completing structural synthesis of the three branches, by selecting three branch chains from the different tables synthesized above and connecting them to the fixed base and the moving platform respectively, a 2R1T-type PM will be built. In order to meet the fully-uncoupled kinematic characteristics for the mechanism, the orientation of the actuated joints mounted on the base should be consistent with the branch assembly requirements. Axes of the rotational joints at the end of the first and second branches should be coaxial and in the same direction as the rotational axis at the end of the third branch. Concurrently, sum of the connectivity of three branches selected should be not more than 15.

For example, by selecting $C_zR_zR_zR_x$ chain in Table 2, $R_zC_xP_mR_x$ chain in Table 3 and P_yU_{xz} chain in Table 4, a new fully-decoupled 2R1T CRRR-RCPR-PU parallel mechanism is generated, shown in Fig. 2.

CRRR-RCPR-PU PM as shown in Fig. 2, the axes of rotational joint (R) and the cylindrical joint (C), which directly connected to the basic platform in the first and the second branches, are parallel to each other and perpendicular to the prismatic joint (P) in the third chain whose axis is parallel to y-axis. The

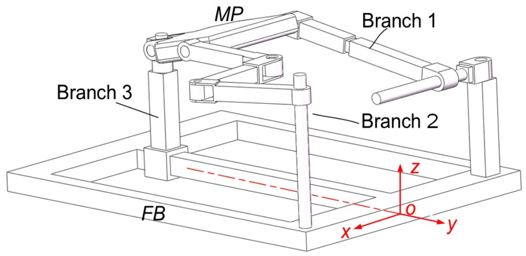

Fig. 2. CRRR-RCPR-PU parallel mechanism.

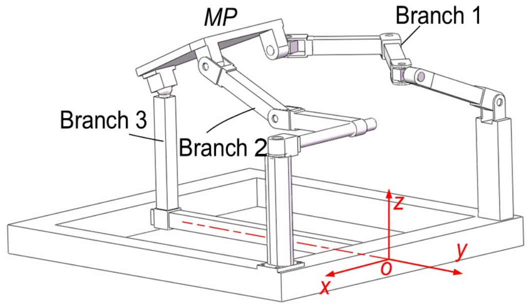

Fig. 3. RURU-RCRR-PS parallel mechanism.

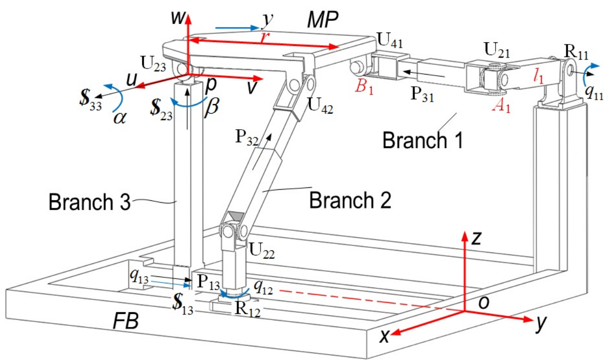

Fig. 4. 2RUPU-PU parallel mechanism.

axes of the rotational joints (R) directly connected to the moving platform in the first and second branches are coaxial and parallel to the rotational joint (R) axis at the end of the third branch.

In the same way, by using the different branch structures, many novel parallel mechanisms can be designed, such as the fully-decoupled 2R1T RURU-RCRR-PS mechanism in Fig. 3, the fully- decoupled 2R1T 2RUPU-PU mechanism in Fig. 4.

RURU-RCRR-PS PM as shown in Fig. 3, in the first and third branches, the axes of the rotational joint and translational joint fixed on the basic platform are parallel to each other. At the same time, both of them are normal to the axis of the first rotational joint in the second branch. Furthermore, axes of the rotational joints connected to the moving platform at the end of the first and second branches are co-axis.

2RUPU-PU PM as shown in Fig. 4, axis of the joint R_{11} is parallel to the pair P_{13}, and normal to the axis of the joint R_{12}, which is parallel to z-axis. In addition, the end-rotational axes of the universal joints U_{41} and U_{42} are co-axis, and parallel to the end-rotational axis of the joint in the third branch.

5. Mobility and kinematics analysis

In this section, 2RUPU-PU PM is preferred (see Fig. 4), and its mobility and kinematics are analyzed.

5.1 Mobility analysis

Establishing the basic coordinate system *o-xyz*, as see in Fig. 4, set the intersection point of the prismatic joint P_{13} axis and the base as the origin o, *y*-axis is coincident with P_{13} axis, *z*-axis is perpendicular to the base. On the platform, the movement coordinate system p-uvw is fixed, origin point *p* is at the rotational center of the universal joint U_{23}, *u*-axis is coincident with the end axis of joint U_{23}, and *w*-axis is normal to the plane of the platform, and *v*-axis can be defined by right hand rule.

Since the kinematic screw systems of both the first and the second branches are 6-system, they do not provide any constraint force to the platform. As for the third branch, the kinematic screw system is written as,

$$\begin{aligned} \$_{13} &= [0 \quad 0 \quad 0; \quad 0 \quad 1 \quad 0]^{\mathrm{T}} \\ \$_{23} &= [0 \quad 0 \quad 1; \quad a_{23} \quad b_{23} \quad 0]^{\mathrm{T}} \\ \$_{33} &= [1 \quad 0 \quad 0; \quad 0 \quad b_{33} \quad c_{33}]^{\mathrm{T}} \end{aligned} \tag{34}$$

where, a_{j3}, b_{j3} and c_{j3} $(j = 2,3)$ are the position parameters of the corresponding joint screw.

Based on the reciprocal product theory, the constraint screws of the third branch are derived as

$$\begin{aligned} \$^r_{13} &= [1 \quad 0 \quad 0; \quad 0 \quad 0 \quad -a_{23}]^{\mathrm{T}} \\ \$^r_{23} &= [0 \quad 0 \quad 1; \quad -c_{33} \quad 0 \quad 0]^{\mathrm{T}} \\ \$^r_{33} &= [0 \quad 0 \quad 0; \quad 0 \quad 1 \quad 0]^{\mathrm{T}} . \end{aligned} \tag{35}$$

Eq. (35) shows that there are two zero-pitch constraint screws and an infinite-pitch constraint screw. They limit the translational DOFs along *x*- and *z*-axis, the rotational DOF around *y*-axis of the platform.

Consequently, the 2RUPU-PU PM can only translate along *y*-axis, rotate around *x*- and *z*-axis.

Meanwhile, calculate the DOF of the mechanism, and

$$M = \lambda(n - g - 1) + \sum_{i=1}^{g} f_i + v - \zeta \tag{36}$$

where, M is the DOF values, λ the order of the mechanism, n the number of components including the base, g the number of joints, f_i is the DOF number of the *i*-th joint, v and ζ represent the numbers of the redundant constraints and the local mobility, respectively.

As the mechanism shown in Fig. 4, λ = 6, n = 9, g = 10, $\sum f_i$ = 15, v = 0 and ζ = 0, then, M = 6(9-10-1)+15 = 3. Therefore, it is a 3-DOF 2R1T parallel mechanism.

5.2 Kinematics analysis

Referring to Fig. 4, let q_{11}, q_{12} and q_{13} are the input parameters of the actuated joints in the three branches, and α, β and y are the output parameters of the moving platform, respectively. Both points A_1 and B_1 are the center of joints U_{21} and U_{41}, respectively.

Provided joint R_{11} in the first branch and joint U_{23} in the third branch have the same height along *z*-axis in coordinate system *o-xyz*. According to the structure of the first branch chain, points A_1 and B_1 always lie in the same horizontal plane. Then, we have

$$r \sin \alpha = l_1 \sin q_{11} \tag{37}$$

where, l_1 is the length of the first branch's actuated link, and *r* is the platform's size.

Based on the third branch, we know that the coordinate value of point *p* on the *y*-axis is equal to the distance between joint P_{13} and point *o*. Then, we have

$$y = q_{13} . \tag{38}$$

Furthermore, in accordance with the second and third branches' assembly requirements, rotational axes connected directly to the platform in the universal joints U_{42} and U_{23}, and the rotational axis adjacent to the joint R_{12} in joint U_{22} are constantly parallel to each other. That implies the rotational angle β around the *z*-axis is equal to the input angular displacement q_{12} of the actuated joint R_{12}, we have

$$\beta = q_{12} . \tag{39}$$

Differentiating Eqs. (37)-(39) with respect to time, and rearranging them into the vector form, yields

$$\boldsymbol{V} = \boldsymbol{J}\dot{\boldsymbol{q}} \tag{40}$$

where, $\boldsymbol{V} = [\omega_u \quad \omega_z \quad v_y]^{\mathrm{T}}$ is the output velocity vector space, $\dot{\boldsymbol{q}} = [\dot{q}_{11} \quad \dot{q}_{12} \quad \dot{q}_{13}]^{\mathrm{T}}$ is the input velocity vector space of the actuated joints, $\boldsymbol{J}$ denotes the Jacobian matrix, and

$$\boldsymbol{J} = \begin{bmatrix} \psi & 0 & 0 \\ 0 & 1 & 0 \\ 0 & 0 & 1 \end{bmatrix} \tag{41}$$

here, $\psi = l_1 \cos q_{11} / (r \cos \alpha)$.

It is obvious that $\boldsymbol{J}$ is a diagonal one, which demonstrates that the velocities of the input and output are in direct correspondence with one another in the correspondence. Therefore, the 2RUPU-PU PM is fully decoupled. The outcome validates the validity and efficacy of the type synthesis approach for full-decoupled 2R1T parallel mechanisms.

6. Conclusions

Type synthesis of parallel mechanisms (PM) is the critically theoretical basis and the source of the innovative design for the mechanical equipment and robots. In this paper, a systematic type synthesis method for the fully-decoupled 2R1T PM is established based on the actuation wrench screw theory. Configuration synthesis and creative design of PMs with the expected motion characteristics are realized by using the method proposed. Kinematic analysis of the 2RUPU-PU PM is carried out. The results show that the mechanism has two- rotational and one-translational DOFs, and its velocity Jacobian matrix is a diagonal one, which indicates that there is a one-to-one mapping relationship between the output and input motions of the PM. Therefore, the mechanism has fully-decoupled kinematic characteristics, which verifies the correctness of the proposed synthesis method of the fully-decoupled 2R1T PM. This kind of mechanisms has the potential applications on the rehabilitation robot, industrial robots, etc. Moreover, the theoretical approach will provide a new way to design the PMs with the different mobility.

Acknowledgments

This work is supported by the Scientific and technological Research Project of Henan Province, China (192102210221).

Nomenclature

$\boldsymbol{T}$: Instantaneous output velocity vector
$\dot{q}_{ji}$: Velocity
$\boldsymbol{\$}_{ji}$: Instantaneous motion screw
F_i : Connectivity of the branch
n : Number of branches
$\boldsymbol{v}$: Linear velocity vector
$\boldsymbol{J}_{dir}$: Direct Jacobian matrix
$\boldsymbol{J}_{inv}$: Inverse Jacobian matrix
α, β, γ : Output parameters
$\boldsymbol{J}$: Jacobian matrix

References

[1] L. W. Tsai, The enumeration of a class of three-dof parallel manipulators, *The 10th World Congress on the Theory of Machine and Mechanisms,* Oulu, Finland (1999) 1121-1126.
[2] T. A. Hess-Coelho, Topological synthesis of a parallel wrist mechanism, *ASME Journal of Mechanical Design*, 128 (1) (2006) 230-235.
[3] Q. C. Li and J. M. Herve, 1T2R parallel mechanisms without parasitic motion, *IEEE Transactions on Robotics*, 26 (3) (2010) 401-410.
[4] J. M. Herve, The mathematical group structure of the set of displacements, *Mechanism and Machine Theory*, 29 (1) (1994) 73-81.
[5] J. Meng, G. F. Liu and Z. X. Li, A geometric theory for analysis and synthesis of Sub-6 DOF parallel manipulators, *IEEE Transactions on Robotics*, 23 (4) (2007) 625-649.
[6] Y. J. Zhou, S. H. Li and J. Sun, Type synthesis approach for the 2R1T compliant parallel mechanism with a suitable constrained branch, *Mechanical Sciences*, 13 (1) (2022) 67-78.
[7] Z. Huang and Q. C. Li, Type synthesis of symmetrical lower-mobility parallel mechanisms using the constraint-synthesis method, *International Journal of Robotics Research*, 22 (1) (2003) 59-79.
[8] G. Gogu, Structural synthesis of full-isotropic translational parallel robots via theory of linear transformations, *European Journal of Mechanics A/Solids*, 23 (2004) 1024-1039.
[9] G. Gogu, Structural synthesis of fully-isotropic parallel robots with Schönflies motions via theory of linear transformations and evolutionary morphology, *European Journal of Mechanics-A/Solids*, 26 (2) (2007) 242-269.
[10] B. Hu and P. Bai, Type synthesis of serial kinematic chains with screw type terminal constraints based on an adding joint method, *Mechanism and Machine Theory*, 184 (2023) 105277.
[11] H. P. Shen, Y. N. Zhao and J. Li, A novel partially-decoupled translational parallel manipulator with symbolic kinematics, singularity identification and workspace determination, *Mechanism and Machine Theory*, 164 (2021) 104388.
[12] H. P. Shen, D. Chablat and B. X. Zeng, A translational three-degrees-of-freedom parallel mechanism with partial motion decoupling and analytic direct kinematics, *Journal of Mechanisms and Robotics*, 12 (2) (2020) 021112.
[13] F. Gao, J. L. Yang and Q. J. Ge, Type synthesis of parallel mechanisms having the second class GF sets and two dimensional rotations, *Journal of Mechanisms and Robotics*, 3 (1) (2011) 011003-1-011003-8.
[14] J. He, F. Gao and X. D. Meng, Type synthesis for 4-DOF parallel press mechanism using GF set theory, *Chinese Journal of Mechanical Engineering*, 28 (4) (2015) 851-859.
[15] Z. M. Chen, Q. X. Xi and F. Gao, Fault-tolerant gait design for quadruped robots with one locked leg using the G(F) set theory, *Mechanism and Machine theory*, 178 (2022) 105069.
[16] X. W. Kong and C. M. Gosselin, Forward displacement analysis of third-class analytic 3-RPR planar parallel manipulators, *Mechanism and Machine Theory*, 36 (9) (2001) 1009-1018.
[17] S. Zarkandi, Kinematic analysis and workspace optimization of a novel 4RPSP+PS parallel manipulator, *Mechanics Based Design of Structures and Machines*, 49 (1) (2020) 131-153.
[18] S. H. Li, Y. X. Shan and J. J. Yu, Actuation spaces synthesis of lower-mobility parallel mechanisms based on screw theory, *Chinese Journal of Mechanical Engineering*, 34 (1) (2021) 1-12.
[19] K. H. Hunt, Structural kinematics of in-parallel- actuated robot-arms, *Journal of Mechanical Design*, 105 (4) (1983) 705-712.
[20] W. Choi and Y. Takeda, Displacement analysis and design of a (2-RRU)-URR parallel mechanism performing 2R1T output

motion for thumb rehabilitation, *Robotics*, 9 (3) (2020) 67.

[21] S. Herreo, C. Pinto and M. Diez, Optimization of the 2PRU-1PRS parallel manipulator based on workspace and power consumption criteria, *Applied Sciences*, 11 (17) (2021) 7770.

[22] T. Sun and X. M. Huo, Type synthesis of 1T2R parallel mechanisms with parasitic motions, *Mechanism and Machine Theory*, 128 (2018) 412-428.

[23] Y. D. Xu, Y. Zhao and Y. Yue, Type synthesis of over-constrained 2R1T parallel mechanisms with the fewest kinematic joints based on the ultimate constraint wrenches, *Mechanism and Machine Theory*, 147 (2020) 103766.

[24] J. H. Qin, C. Z. Yu and Z. B. Sun, A novel method for type synthesis of parallel mechanism without parasitic motion based on 2R1T parallel mechanism with rotational bifurcation, *Chinese Journal of Mechanical Engineering*, 35 (1) (2022) 1-12.

[25] Z. Wu, Q. C. Li and Y. Wei, Design of a new family of kinematically redundant parallel mechanisms with two rotations and one translation, *Journal of Mechanical Design*, 145 (5) (2023) 053303.

[26] G. Gogu, Fully-isotropic T1R2-type parallel robots with three degrees of freedom, *Proceedings of the ASME International Design Engineering Technical Conferences and Computers and Information in Engineering Conferences - DETC2005*, Long Beach, CA, USA (2005) 757-764.

[27] G. Gogu, Fully-isotropic parallel robots with four degrees of freedom T2R2-type, *Proceedings of IEEE/RSJ International Conference on Intelligent Robots and Systems (IROS 2005)*, Edmonton, Canada (2005) 1190-1195.

[28] M. Carricato, Fully-isotropic four degrees-of- freedom parallel mechanisms for schöenflies motion, *International Journal Robotics Research*, 24 (5) (2005) 397-414.

[29] C. H. Kuo and J. S. Dai, Structure synthesis of a class of parallel manipulators with fully decoupled projective motion, *Journal of Mechanisms and Robotics*, 13 (3) (2021) 031011.

[30] Y. B. Zhang, X. L. Jing and J. H. Han, Type synthesis of uncoupled rotational parallel mechanisms with two degrees of freedom, *Journal of Mechanical Engineering*, 54 (15) (2018) 21-30.

[31] Y. B. Zhang, Y. F. Zhao and X. L. Jing, Type synthesis of uncoupled translational parallel manipulators based on actuation wrench screw theory, *Advances in Mechanical Engineering*, 10 (1) (2018) 1-10.

[32] C. H. Kuo and J. S. Dai, Kinematics of a fully-decoupled remote center-of-motion parallel manipulator for minimally invasive surgery, *Journal of Medical Devices*, 6 (2) (2012) 211-214.

[33] T. C. Chang and X. D. Zhang, Kinematics and reliable analysis of decoupled parallel mechanism for ankle rehabilitation, *Microelectronics Reliability*, 99 (2019) 203-212.

[34] C. Zhang and Y. Song, Design and kinematic analysis of a novel decoupled 3D ultrasonic elliptical vibration assisted cutting mechanism, *Ultrasonics*, 95 (2019) 79-94.

Yanbin Zhang, born in 1974, is a Professor in School of Mechatonics Engineering, Henan University of Science and Technology. He received his Ph.D. in Mechanical Engineering from Xi'an University of Technology. His research interests include parallel mechanism theory and rehabilitation robot technology.

E-mail: yanbin_zh@haust.edu.cn

Xuemin Wei, born in 1998, is a master student in School of Mechatonics Engineering, Henan University of Science and Technology. Her research interests include parallel mechanism theory.